International Journal of Non-Linear Mechanics 43 (2008) 1108 – 1120

Contents lists available at ScienceDirect

International Journal of Non-Linear Mechanics

journal homepage: www.elsevier.com/locate/nlm

The stochastic elastica and excluded-volume perturbations of DNA conformational ensembles

Gregory S. Chirikjian

Department of Mechanical Engineering, Johns Hopkins University, Baltimore, MD 21218, USA

ARTICLE INFO

Article history:
Received 7 November 2007
Received in revised form 1 September 2008
Accepted 13 October 2008

Keywords:
DNA
Conformation
Ensemble
Convolution
Lie group
Excluded volume
Probability density function

ABSTRACT

A coordinate-free Lie-group formulation for generating ensembles of DNA conformations in solution is presented. In this formulation, stochastic differential equations define sample paths on the Euclidean motion group. The ensemble of these paths exhibits the same behavior as solutions of the Fokker–Planck equation for the stochastically forced elastica. Longer chains for which the effects of excluded volume become important are handled by piecing together shorter chains and modeling their interactions. It is assumed that the final chain lengths of interest are long enough for excluded-volume effects to become important, but not so long that the semi-flexible nature of the chain is lost. The effect of excluded volume is then taken into account by grouping short self-avoiding conformations into "bundles" with common end constraints and computing average interaction effects between bundles. The accuracy of this approximation is shown to be good when using a numerically generated ensemble of self-avoiding sample paths as the baseline for comparison.

1. Introduction

This section presents an overview of the major results of this paper together with a review of the literature on DNA statistical mechanics.

1.1. Overview

This paper makes several contributions to the study of equilibrium fluctuations of DNA conformations:

- A model of DNA fluctuations using a stochastic differential equation (SDE) on the group of rigid-body motions is developed. This model relates the magnitude of the stochastic forcing to the temperature and stiffness of the elastic-filament model of DNA. In one version of this model, excluded-volume effects[1] are taken into account explicitly by weeding out conformations that have self-interpenetration of sequentially distant base pairs.
- The relationship between the SDE model and the corresponding Fokker–Planck equation is explained. The latter generates a probability density function (pdf) describing the distribution of relative position and orientation of reference frames attached to base pairs at any two different values of arc length. For short semi-flexible chains, excluded volume is not an important effect because short chains cannot bend back enough to allow interpenetration. Therefore, the Fokker–Planck approach can be used to generate valid statistics for short segments.
- The probability densities obtained from the Fokker–Planck approach can be "pieced together" by performing a convolution operation of the probability densities corresponding to two consecutive segments. This convolution is an integral over the group of rigid-body motions. When the segment resulting from the concatenation of two short segments is itself short enough that no interactions result, the convolution approach is exact. However, for longer segments, the convolution must be modified to take into account interactions between segments. A model for performing this modification is introduced in this paper.
- The concept of "conformational bundles" is introduced as a way to approximate the average effects of interaction between two adjacent segments, each of which is described by an ensemble of conformations that have a common end constraint in position and orientation.
- Numerical studies are performed to evaluate the results of the quasi-closed-form conformational bundles approach against the SDE approach in which sample paths are generated and

E-mail address: gregc@jhu.edu.

[1] The excluded-volume effect is essentially a statement of the fact that two masses cannot occupy the same space at the same time, and this imposes a constraint that polymer conformations must be self-avoiding.

0020-7462/$ - see front matter © 2008 Published by Elsevier Ltd.
doi:10.1016/j.ijnonlinmec.2008.10.005

self-intersecting conformations are removed. This is done for a variety of filament thicknesses.

In the following section a brief review of the vast literature on DNA mechanics and statistical fluctuations is provided.

1.2. Literature review

The theory of semi-flexible/worm-like polymer chains originated more than fifty years ago [1–3]. Since then, the statistical mechanics of chains such as DNA has received substantial attention in the literature. Now-classical polymer-theoretic references include [4–9]. Studies devoted to ring-closure probabilities include [10,11]. Modeling works in the past 20 years include [12–21]. In particular, Brownian dynamics is a tool that is often used to relate theory and experimental data (see discussions in [22–24]). And semi-flexible polymer theories based on diffusion processes can be found in [25–28]. Excluded-volume effects in polymer solutions in general [29,30], and for semi-flexible chains in particular [31] have been studied. The main approaches are the use of renormalization group concepts [32,33] and mean field potentials [29,34].

In these theories, the pdf describing the relative frequency of occurrence of positions and orientations of the distal end of the chain for given position and orientation of the proximal end play an important role [29,30,32,35–37]. And a number of new theoretical models have been developed by the author's group for generating this quantity from given stiffness models [38–42].

Experimental measurements of DNA stiffness parameters have been reported in [37,43–47]. Efforts to characterize integrals of the joint positional and orientational pdf over many of its arguments can be found in [11,48], and the whole distribution in the case of the helical worm-like chain can be found in [37]. DNA elastic properties and experimental measurements of DNA elastic properties such as twist/stretch coupling have been reported in [49–55].

Elastic models of DNA mechanics has a long history [56,57]. A number of recent studies on chiral and uncoupled end-constrained elastic rod models of DNA with circular cross-section have been presented [58–61]. These models use classical elasticity theory of continuum filaments with or without self-contact constraints to model the stable conformations of DNA in plasmids, in chromosomes, and during transcription.

In some works, Euler angles are used in parameterizing equations of the Kirchhoff elastic rod theory to obtain equilibrium conformations of DNA and determine its stability [62–64]. Also, the worm-like chain model has been used to model the equilibrium behavior of DNA [65]. More recent works involve the modeling of DNA as an anisotropic inextensible rod and also include the effect of electrostatic repulsion for describing the DNA loops bound to Lac repressor, etc. [66,67]. Another recent work includes sequence-dependent elastic properties of DNA [68]. All of these aforementioned works are based on Kirchhoff's thin elastic rod theory [69]. This theory, as originally formulated, deals with non-chiral elastic rods with circular cross-section. Another example is the special Cosserat theory of rods [70], which can be viewed as an extension of Kirchhoff's theory in that it includes extensible and shearable rods. Several researchers in elasticity have employed this rod theory to describe the static and dynamic characteristics of rods. For example, Simo and Vu-Quoc formulated a finite element method using rod theory [71]. Dichmann et al. employed a Hamiltonian formulation using the special Cosserat theory of rods for the purpose of describing DNA [72]. Coleman et al. reviewed dynamical equations in the theories of Kirchhoff and Clebsch [73]. Steigmann and Faulkner derived the equations of classical rod theory using parameter-dependent variational approach [74]. Recently, Gonzalez and Maddocks devised a method to extract sequence-dependent parameters for a rigid base-pair DNA model from molecular dynamics simulation [75]. In their paper, they used a force moment balance equation from Kirchhoff's rod theory to extract stiffness and inertia parameters. Another recent work includes the application of Kirchhoff rod theory to marine cable loop formation and DNA loop formation [76]. Recently, Wiggins et al. developed a theory based on non-linear elasticity, called kinkable worm-like chain model, for describing spontaneous kinking of polymers including DNA [77].

The approach taken in this paper is to apply a new kind of statistical treatment of semi-flexible chains that starts with the solution of diffusion equations, yet includes the effects of excluded volume. The key to this approach is the use of the concept of "conformational bundles", which were introduced in [42], and are used here for the first time in the context of semi-flexible polymers.

1.3. Organization of the remainder of the paper

The remainder of this paper is structured as follows: Section 2 reviews the concept of a frame distribution function for semi-flexible chains, which was introduced by the author in previous work. Section 3 explains how frame distribution functions can be computed accurately using diffusion equations for chain lengths of less than two persistence lengths. For longer chains, an ensemble of sample paths generated from a SDE has equivalent statistics as those produced by the diffusion equations before self-intersecting conformations are removed. The obvious advantage of the SDE approach is that self-intersecting conformations can be explicitly removed from the ensemble thereby obtaining statistics for self-avoiding chains. However, this comes at a high computational cost. Section 4 develops the concept of conformational bundles and derives equations relating conformational bundles to frame distributions. The application of the conformational bundle concept to the approximation of excluded-volume effects is formulated in Section 5. In Section 6, analytical and computational examples based on the mathematical formulation of this paper are presented. Section 7 presents conclusions. An Appendix that reviews some relevant mathematical concepts is also included.

2. Functions of rigid-body motion

This section reviews the concept of a function of rigid-body motion and introduces the mathematical tools and notation required to compute coordinate-free derivatives of functions of motion. To begin, a review of rigid-body motions is provided.

2.1. Rigid-body motions

An arbitrary rigid-body motion can be viewed as the pair $g=(R,\mathbf{r})$ where $R \in SO(3)$ (i.e., R is a 3×3 rotation matrix), and $\mathbf{r} \in \mathbb{R}^3$ is a translation vector in three-dimensional space. The identity (or null motion) is $e=(I,\mathbf{0})$ where I is the 3×3 identity matrix. The composition law is $g_1 \circ g_2 = (R_1R_2, R_1\mathbf{r}_2+\mathbf{r}_1)$ and the inverse of each element g is $g^{-1}=(R^{\mathrm{T}}, -R^{\mathrm{T}}\mathbf{r})$. The action of the motion g on a position vector $\mathbf{x}\in\mathbb{R}^3$ is $g\cdot\mathbf{x}=R\mathbf{x}+\mathbf{r}$. (Note the distinction that $\circ$ is used between group elements and $\cdot$ is used between a group element and a vector.) Any g describes the positional and orientational relationship between two reference frames. It is sometimes convenient to refer to the result of a rigid-body motion at a particular time as a "pose," and to refer to a function of motion as a pose distribution.

The collection of all rigid-body motions is denoted in this paper as $G=SE(3)$. (The special Euclidean motion group in three space.) Any $g\in G$ can be faithfully represented with a 4×4 *homogeneous*

transformation matrix of the form:

$$H(g)=\begin{pmatrix} R & \mathbf{r} \\ \mathbf{0}^{\mathrm{T}} & 1 \end{pmatrix}$$

in the sense that $H(g_1 \circ g_2) = H(g_1)H(g_2)$ (i.e., the matrix product of $H(g_1)$ and $H(g_2)$). Here $\mathbf{0}^{\mathrm{T}} = [0,0,0]$ and 1 is the number one. The structure of this bottom row is preserved under multiplication by matrices of the same kind.

Henceforth no distinction is made between G and the set of all 4×4 homogeneous transformation matrices with operation of matrix multiplication. That is, g and $H(g)$ will be used interchangeably, and since the group operator can be viewed as matrix multiplication, it does not need to be written explicitly as $\circ$.

2.2. Positional and orientational distribution functions

A real-valued function of rigid-body motion is denoted as $f(g)$. Such functions arise in a variety of applications. For example, a liquid crystal is made up of many copies of the same essentially rigid molecule. If a reference frame is attached to the center of mass of each molecule with the axes of the frame pointing along the principal axes of inertia, then the distribution of positions and orientations of the molecules relative to a frame that is fixed in space can be recorded and summarized with a pdf of the form $f(g)$. If the situation is dynamic, then the pdf will depend on time in addition to depending on g, which can be written as $f(g;t)$. Here the semicolon is used to separate spatial and temporal variables.

In the context of the equilibrium statistical mechanics of DNA, there is no time variable. Reference frames are attached to the DNA along its length. For example, this can be done by placing the origin of each frame at the center of mass of each base pair, with the local z (or $\mathbf{e}_3$) axis pointing along the tangent to the backbone curve, and the local x (or $\mathbf{e}_1$) axis pointing along the largest principal axis of the base pairs. If the DNA backbone curve is parameterized with curve parameter $s \in [0, L]$, then a function $f(g; s_1, s_2)$ with $s_1 < s_2$ denotes the relative distribution of positions and orientations at $s = s_2$ relative to the frame fixed at $s = s_1$. In inextensible models of DNA, s will denote the arc length. However, it can be the case that a DNA molecule stretches, in which case s will not be the arc length. This issue is discussed later in this section. But first, it is important to review the properties of infinitesimal rigid-body motion. In this context it will be convenient to retain the concept of time, though the independent variable t will be replaced with s when discussing DNA.

2.3. Infinitesimal motions and exponential coordinates

Given a one-parameter motion $g(t)$, we can define the six-dimensional velocity of the rigid-body motion as observed in the moving frame as the non-trivial entries in the matrix

$$g^{-1}\dot{g}=\begin{pmatrix} R^{\mathrm{T}}\dot{R} & R^{\mathrm{T}}\dot{\mathbf{r}} \\ \mathbf{0}^{\mathrm{T}} & 0 \end{pmatrix} \quad \text{where } R^{\mathrm{T}}\dot{R}=\begin{pmatrix} 0 & -\omega_3 & \omega_2 \\ \omega_3 & 0 & -\omega_1 \\ -\omega_2 & \omega_1 & 0 \end{pmatrix}.$$

Here t can be thought of as time, and a dot denotes differentiation with respect to t. Elsewhere in the paper the independent variable is not time, but rather arc length.

Since $R^{\mathrm{T}}\dot{R}$ is skew symmetric as a result of R being orthogonal, it only has three independent non-zero entries. These can be extracted and used to form the dual vector $\boldsymbol{\omega}(t) = [\omega_1(t), \omega_2(t), \omega_3(t)]^{\mathrm{T}}$, which is the angular velocity of the moving frame as seen in the moving frame. In some contexts it will be convenient to write this as $\boldsymbol{\omega}_r(t)$ to distinguish it from the dual vector of $\dot{R}R^{\mathrm{T}}$, which we will call $\boldsymbol{\omega}_l(t)$. These are related as $\boldsymbol{\omega}_l(t) = R\boldsymbol{\omega}_r(t)$.

The independent information in the matrix $g^{-1}\dot{g}$ can be extracted and put in a six-dimensional vector defined as

$$\boldsymbol{\xi}(t)=(g^{-1}\dot{g})^{\vee}=\begin{pmatrix} \boldsymbol{\omega} \\ R^{\mathrm{T}}\dot{\mathbf{r}} \end{pmatrix}.$$

The opposite operation of $\vee$ is $\wedge$:

$$\hat{\boldsymbol{\xi}}(t)=g^{-1}\dot{g}=\sum_{i=1}^{6}\xi_i X_i,$$

where basis elements for the Lie algebra of G (which are also called generators of G) are

$$X_1=\begin{pmatrix} 0 & 0 & 0 & 0 \\ 0 & 0 & -1 & 0 \\ 0 & 1 & 0 & 0 \\ 0 & 0 & 0 & 0 \end{pmatrix}, \quad X_2=\begin{pmatrix} 0 & 0 & 1 & 0 \\ 0 & 0 & 0 & 0 \\ -1 & 0 & 0 & 0 \\ 0 & 0 & 0 & 0 \end{pmatrix},$$

$$X_3=\begin{pmatrix} 0 & -1 & 0 & 0 \\ 1 & 0 & 0 & 0 \\ 0 & 0 & 0 & 0 \\ 0 & 0 & 0 & 0 \end{pmatrix}, \quad X_4=\begin{pmatrix} 0 & 0 & 0 & 1 \\ 0 & 0 & 0 & 0 \\ 0 & 0 & 0 & 0 \\ 0 & 0 & 0 & 0 \end{pmatrix},$$

$$X_5=\begin{pmatrix} 0 & 0 & 0 & 0 \\ 0 & 0 & 0 & 1 \\ 0 & 0 & 0 & 0 \\ 0 & 0 & 0 & 0 \end{pmatrix}, \quad X_6=\begin{pmatrix} 0 & 0 & 0 & 0 \\ 0 & 0 & 0 & 0 \\ 0 & 0 & 0 & 1 \\ 0 & 0 & 0 & 0 \end{pmatrix}.$$

These correspond to infinitesimal rotations and translations about the 1, 2, and 3 axes and form a basis for the Lie algebra associated with G. Matrix exponentiation of any weighted sum of these basis elements produces elements of G. For example,

$$\exp(\theta X_3 + zX_6)=\begin{pmatrix} \cos\theta & -\sin\theta & 0 & 0 \\ \sin\theta & \cos\theta & 0 & 0 \\ 0 & 0 & 1 & z \\ 0 & 0 & 0 & 1 \end{pmatrix}.$$

Furthermore, for small values of θ and z, the matrix exponential is approximated well as

$$\exp(\theta X_3 + zX_6) \approx I + \theta X_3 + zX_6.$$

More generally, any rigid-body motion can be parameterized in either of the forms:

$$g=\exp\left(\sum_{i=1}^{6}x_i X_i\right)=\exp\left(\sum_{i=4}^{6}y_i X_i\right)\exp\left(\sum_{i=1}^{3}y_i X_i\right). \tag{1}$$

The matrix logarithm can be used to convert group elements to Lie algebra elements, and it is convenient to define

$$\mathbf{x}=(\log g)^{\vee}=[x_1,\ldots,x_6]^{\mathrm{T}}.$$

The norm $\|\mathbf{x}\| = \sqrt{\mathbf{x}\cdot\mathbf{x}}$ is a measure of distance from the identity. Near the identity, $\|\mathbf{x}\| \ll 1$ and $x_i \approx y_i$. It can be shown that

$$(\dot{g}g^{-1})^{\vee} \approx (g^{-1}\dot{g})^{\vee} \approx \dot{\mathbf{x}} \approx \dot{\mathbf{y}} \quad \text{when } \|\mathbf{x}\| \ll 1. \tag{2}$$

This is not true when $\|\mathbf{x}\|$ is large, but this property makes these parameterizations useful for describing small motions around the identity.

2.4. Derivatives of functions of motion

Given a smooth function $f(g)$ where $g \in G$, the Lie derivatives from the right and left are defined as

$$\tilde{X}_i^r f(g)=\left.\frac{\mathrm{d}f(g\circ\exp(tX_i))}{\mathrm{d}t}\right|_{t=0} \quad \text{and} \quad \tilde{X}_i^l f(g)=\left.\frac{\mathrm{d}f(\exp(-tX_i)\circ g)}{\mathrm{d}t}\right|_{t=0} \tag{3}$$

for the motion group where $g \in G$ is described using 4×4 transformation matrices. The "r" in the symbol $\tilde{X}_i^r$ is used to denote the position of $\exp(tX_i)$ on the "right side" of g inside the function $f(\cdot)$, and similarly for "l". $\tilde{X}_i^r$ commutes with left shifts of the form $(L(g_1)f)(g)=f(g_1^{-1}\circ g)$, and $\tilde{X}_i^l$ commutes with right shifts of the form $(R(g_1)f)(g)=f(g\circ g_1)$. The operators defined in (3) are analogous to partial derivatives of a function $\phi(\mathbf{x})$ where $\mathbf{x}\in\mathbb{R}^n$ that can be defined as

$$\frac{\partial\phi}{\partial x_i}=\frac{\mathrm{d}}{\mathrm{d}t}\phi(\mathbf{x}+t\mathbf{e}_i)\Big|_{t=0}.$$

The explicit form of the Lie derivative operators in (3) in terms of coordinate descriptions are given in Appendix A.

3. The stochastic elastica

In this section the relationship between the stochastic elastica and diffusion equations on the group of rigid-body motions is established. Section 3.1 introduces the stochastic elastica. Section 3.2 explains the relationship between the strength of the noise and the stiffness of the elastic filament. Section 3.3 formulates the problem of finding the probability density of position and orientation of the distal end of an elastica relative to its proximal end when it is subjected to Brownian motion forcing from the environment. This is a "phantom" model in which the effects of excluded volume are not considered. Section 3.4 compares and contrasts the SDE and Fokker–Planck approaches. Modifications of these models that include excluded-volume effects are discussed later in the paper.

3.1. A model based on SDE

The classical elastica (elastic filament) problem goes back to Euler, and was addressed in detail by Kirchhoff and Clebsch in the 19th century, and summarized in Love's classical treatment of elasticity [69]. In the current context a stochastic version of the problem is developed as a model for the equilibrium fluctuations of DNA.

The preferred (or referential) conformation of the DNA can be defined infinitesimally as $\xi(s)=\xi_0(s)$. Integrating the ODE $\mathrm{d}g/\mathrm{d}s=g\hat{\xi}(s)$ for $s\in[0,L]$ subject to the initial conditions $g(0)=e$ then defines a framed curve that describes DNA conformation. In particular, $\xi_0(s)$ defines the referential conformation that minimizes the elastic energy of deformation of the filament. The referential conformation is the shape that the DNA backbone would adopt as the temperature slowly approaches absolute zero and all thermal fluctuations vanish. For example, if $\xi_0(s)$ is a constant vector, then the resulting backbone curve will be a helix. While this constant case corresponds to the standard form of DNA, keeping the formulation more general allows for cases in which the DNA has internal bends or kinks, such as would be the case when transcription factors bind [78,79].

The relationship between s and arc length, $l(s)$, is

$$l(s)=\int_0^s\sqrt{\xi_4^2(\sigma)+\xi_5^2(\sigma)+\xi_6^2(\sigma)}\,\mathrm{d}\sigma.$$

In inextensible and shearless models of DNA, it is automatically true that $l(s)=s$. And while the current formulation is not limited to this case, it will be convenient to think of s as arc length. Consider an infinitesimal segment of the backbone curve of DNA between s and $s+\mathrm{d}s$. Rather than observing the equality $\xi(s)=\xi_0(s)$, a stochastically forced elastica would satisfy an equation of the form:

$$\xi(s)\,\mathrm{d}s=\xi_0(s)\,\mathrm{d}s+B(s)\,\mathrm{d}\mathbf{W}, \tag{4}$$

where $\mathbf{W}(s)$ is a vector of uncorrelated unit strength Wiener processes that reflect that the infinitesimal segment of the DNA is being forced by the Brownian motion of the surrounding solvent. Eq. (4) results from a force balance in the case when the inertia is considered to be negligible. It is a SDE on the Lie algebra of G. Analogous equations (with s replaced by t) have been used in the non-inertial theory of rotational and translational Brownian motion of rigid molecules [80,81]. The exact form of the coloring matrix $B(s)$ for the case of DNA will be determined shortly.

If we integrate the corresponding Stratonovich SDE $\mathrm{d}g=g\hat{\xi}(s)\,\mathrm{d}s$ to find $g(s)$ for $s\in[0,L]$, and we do this many times to obtain an ensemble of sample paths, the recorded statistics of this ensemble will result in the set of normalized histograms (i.e., probability densities) $f(g;0,s)$ for $s=[0,L]$. The general theory of Brownian motions on Lie groups "injected" from Lie algebras provides the mathematical machinery to obtain $f(g;0,s)$ directly without sampling [41,82]. This will be discussed later in the paper.

3.2. Relating $B(s)$ to the stiffness of the filament

A non-uniform extensible elastic filament with unstretched length L has elastic energy of the form

$$E_1=\int_0^L F(\xi(s),s)\,\mathrm{d}s, \tag{5}$$

where

$$F(\xi(s),s)=\tfrac{1}{2}[\xi(s)-\xi_0(s)]^{\mathrm{T}}K(s)[\xi(s)-\xi_0(s)].$$

Here $\xi_0(s)$ defines the minimal energy conformation and $K(s)=K^{\mathrm{T}}(s)\in\mathbb{R}^{6\times6}$ is a positive definite stiffness matrix that defines the resistance to the backbone to bending, twisting, extension and shear deformations. As mentioned earlier, given $\xi_0(s)$, it is possible to integrate the matrix differential equation

$$\frac{\mathrm{d}g_0}{\mathrm{d}s}(s)=g_0(s)\hat{\xi}_0(s)$$

subject to the initial condition $g(0)=e$ (the 4×4 identity matrix) for $s\in[0,L]$ to obtain the minimal energy conformation rooted at the identity.

Here, as in the rest of the paper, the independent variable is the curve parameter, s, rather than time, t. The curve parameter s is taken to be the arc length of the filament in its undeformed (referential) conformation $g_0(s)$. This may or may not be the arc length of the filament after a deformation, depending on whether or not it stretches.

Consider a very short chain defined by $L=\Delta s$ in (5). Over this very short range $K(s)$ is effectively constant. Furthermore, since $g(0)=e$, it follows from (2) that $\xi(s)\approx\dot{\mathbf{x}}$. This means that the potential energy in (5) resembles the kinetic energy of a body with a generalized inertia matrix K, when s is viewed as time. The Boltzmann distribution corresponding to such a quadratic energy functional is a Gaussian distribution with covariance of the form $\Sigma=(k_BT)K^{-1}$ where k_B is the Boltzmann constant and T is the absolute temperature.

In contrast, the mean and covariance of the ensemble of sample paths generated from the SDE in (4) can be computed for short segments defined by $s\in[0,\Delta s]$ as

$$\langle\xi(s)\rangle=\xi_0(s)\quad\text{and}\quad\langle[\xi(s)-\xi_0(s)][\xi(s)-\xi_0(s)]^{\mathrm{T}}\rangle=B(s)B^{\mathrm{T}}(s).$$

The matrix BB^{T} can be denoted as D, which is the diffusion matrix for the system. Matching the covariances indicates that

$$D(s)=B(s)B^{\mathrm{T}}(s)=(k_BT)K^{-1}(s). \tag{6}$$

In other words, the diffusion matrix, D, is proportional to both the temperature and the inverse of the stiffness matrix. As temperature increases, there is more diffusion for a fixed stiffness matrix. Or if the temperature is fixed, then diffusion increases for more flexible (less stiff) chains. While the calibration in (6) was for an infinitesimal

segment of the backbone curve, the result impacts the positional and orientational distribution of reference frames that are far away from each other as measured in terms of arc length.

3.3. The Fokker–Planck approach

Corresponding to any SDE is a partial differential equation, called the Fokker–Planck equation [83,84] (also called the forward Kolmogorov equation [85]), that describes the evolution of probability density in the variables of the SDE. The ensemble of paths $\{g(s)|s \in [0,L]\}$ generated by the SDE in the previous subsections can be used to approximate $f(g;0,s)$ for $s=[0,L]$ by generating samples and forming a histogram. In the limit as the number of samples approaches infinity, $f(g;0,s)$ generated in that way would approach the solution of the corresponding Fokker–Planck equation, which is a PDE in both s and the variables that parameterize g. The derivation of the Fokker–Planck equation corresponding to any SDE is well-known, but is rather involved. See the following for derivations [41,82,86,87]. Using that methodology, the particular Fokker–Planck equation corresponding to the SDE in (4) with (6) is

$$\frac{\partial f}{\partial s} = \frac{1}{2}\sum_{k,l=1}^{6} D_{lk}(s)\tilde{X}_l^r\tilde{X}_k^r f - \sum_{l=1}^{6}(\boldsymbol{\xi}_0(s)\cdot\mathbf{e}_l)\tilde{X}_l^r f \tag{7}$$

subject to the initial conditions

$$f(g;0,0)=\delta(g).$$

Note that an alternative derivation of (7) can be obtained using path-integral techniques [37,38,88]. Here $\tilde{X}_k^r$ are the Lie derivative operators defined in (3). Eq. (7) takes into account anisotropy and inhomogeneity of the elasticity (which has been observed in, e.g. [89]), as well as arbitrary minimal energy shape, and has essentially the same derivation as the homogeneous case presented in [38–40]. A single pose distribution is illustrated with level curves in Fig. 1(a) along with several sample paths. Of course, it is really a six-dimensional distribution that cannot be visualized, but one can think of it as depicted in Fig. 1(a).

Under the extreme condition that $T \to 0$, no diffusion would take place, and $f(g;,0,s) \to \delta(g_0^{-1}(s)\circ g)$. For the biologically relevant case ($T \approx 300$), (7) can be solved using the harmonic analysis approach in [38–40]. If we make the shorthand notation $f_{s_1,s_2}(g)=f(g;s_1,s_2)$, then it will always be the case for $s_1<s<s_2$ that

$$f_{s_1,s_2}(g)=(f_{s_1,s}*f_{s,s_2})(g)=\int_G f_{s_1,s}(h)f_{s,s_2}(h^{-1}\circ g)\,\mathrm{d}h. \tag{8}$$

This is the six-dimensional convolution integral of two pose distributions. Here h is a dummy variable of integration, and the explicit form of the invariant integration measure, dh, is reviewed in Appendix A. While (8) will always hold for semi-flexible phantom chains, for the homogenous case (where D and $\boldsymbol{\xi}_0$ are independent of s) there are the additional convenient properties:

$$f(g;s_1,s_2)=f(g;0,s_2-s_1) \quad \text{and} \quad f(g;s_2,s_1)=f(g^{-1},s_1,s_2). \tag{9}$$

The first of these says that for a uniform chain the pose distribution only depends on the difference of arc length along the chain. The second provides a relationship between: (a) the pose distribution for a uniform chain resulting from taking the frame at s_1 to be fixed at the identity and recording the poses visited by s_2; and (b) the distribution of frames at $s=s_1$ that results when s_2 is fixed at the identity. However, neither of these nor (8) will hold when excluded-volume interactions are taken into account. Later in the paper we consider how the convolution in (8) must be modified when taking into account excluded volume.

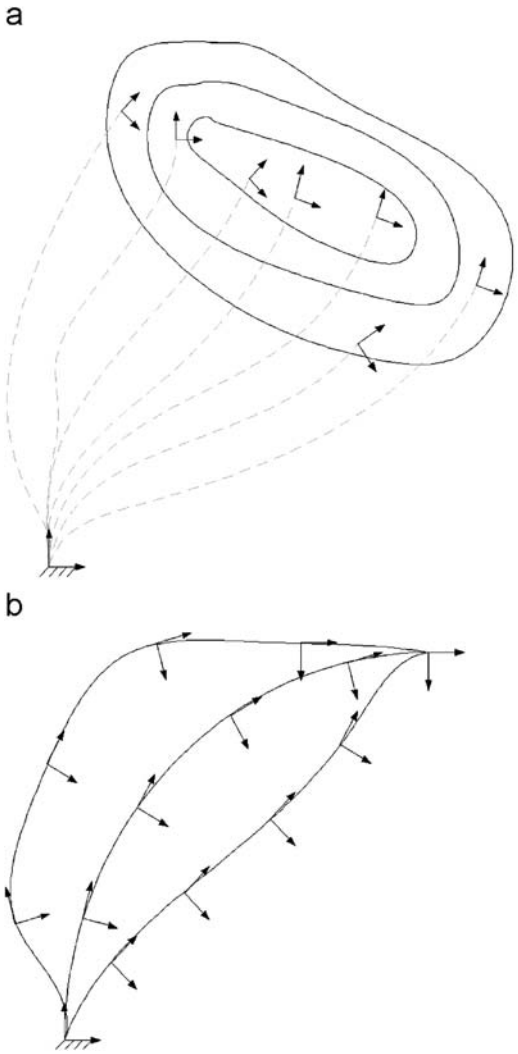

Fig. 1. The functions $f(g_1;0,L)$ and $m(g_1,g;0,L)$: here g_1 denotes the pose of the frame located at the end of the segment of length L. If g_1 is held fixed $m(g_1,g;0,L)$ is the probability that some filament in the bundle will have a pose g where each point on each fiber in the bundle is described by $s \in [0,L]$. (a) The function $f(g_1;0,L)$: the probability density function of end positions and orientations of a semi-flexible polymer defined by arclength in the range from 0 to L with base fixed at the identity reference frame e and distal end free to visit any $g_1 \in G$. (b) The function $m(g_1,g;0,L)$ describing the distribution of all reference frames attached to all conformations of a chain defined by arclength in the range from 0 to L with base fixed at e and distal end fixed at g_1.

As a specific example of when $f(g;s_1,s_2)=f(g;0,s_2-s_1)$, if the chain is uniform, inextensible and shearless, the constant diffusion matrix will be of the form

$$D=\begin{pmatrix} D_{11} & D_{12} & D_{13} & 0 & 0 & 0 \\ D_{12} & D_{22} & D_{23} & 0 & 0 & 0 \\ D_{13} & D_{23} & D_{33} & 0 & 0 & 0 \\ 0 & 0 & 0 & 0 & 0 & 0 \\ 0 & 0 & 0 & 0 & 0 & 0 \\ 0 & 0 & 0 & 0 & 0 & 0 \end{pmatrix}.$$

The lower right block of zeros corresponds to infinite stiffness in shear and stretch.

If the minimal energy conformation is an arc-length-parameterized helix, the drift vector will be constant and of the form

$$\boldsymbol{\xi}_0^{\mathrm{T}}=[\omega_1,\omega_2,\omega_3,0,0,1]^{\mathrm{T}}.$$

In this case (7) is a *degenerate diffusion* on $G = SE(3)$ with constant coefficients. Methods for solving such equations are presented in [38–40]. These methods use the concept of the non-commutative Fourier transform for the Euclidean group. This builds on the work of Miller [90].

Let the evolution of the probability density of relative pose of reference frames attached to a stochastic elastica at values of curve parameter 0 and s be denoted as $f(g;0,s)$. Since it is a probability density, by definition

$$\int_G f(g;0,s)\,\mathrm{d}g = 1. \tag{10}$$

3.4. Comparison of SDE and Fokker–Planck approaches

The benefit of taking an SDE approach is that one can handle the effects of excluded volume at the level of individual conformations/sample paths (whereas the diffusion equation allows all conformations including self-intersecting ones). On the one hand, it is clear that self-intersecting conformations are not desirable in a realistic ensemble. On the other hand, it may not be obvious a priori that a sampling approach which simply "throws away" self-intersecting conformations will be valid. The following argument justifies the approach of removing sample paths that self-intersect.

Imagine that all of the infinite number of possible conformations of the semi-flexible chain (both self-avoiding and self-intersecting) could be enumerated. Each one can be assigned an energy that takes into account both local deformations (which are reflected in the structure of the stiffness matrix $K(s)$) and non-local contacts/interpenetration of points that are distal in arc length.

The equilibrium ensemble will be described by Boltzmann weighted statistics involving the negative of the exponential of the energy normalized by k_BT. The model used here is one in which the energy of interaction between distal points in arc length is either zero when there is no corporeal overlap, or very high when there is an overlap. Therefore the contribution of all self-intersecting conformations is effectively set to zero in the Boltzmann ensemble because the exponential of the negative of a large number is effectively zero. This has the effect of killing all sampled conformations with overlaps, as well as those that are highly deformed from their referential conformation.

The SDE approach is a way to generate conformations that are a priori weighted in the correct way by local energy considerations. But the SDE by itself does not take into account the interactions that are non-local in sequence. Therefore, since

$$\exp(-(E_{local}+E_{non\text{-}local})/k_BT) = \exp(-E_{local}/k_BT)\exp(-E_{non\text{-}local}/k_BT)$$

with $\exp(-E_{non\text{-}local}/k_BT)$ taking a value of 1 when $E_{non\text{-}local}$ is zero (corresponding to no overlap) and $\exp(-E_{non\text{-}local}/k_BT)$ is 0 for an overlap (since $E_{non\text{-}local}$ is very large and positive when there is an overlap), this is equivalent to modifying the Boltzmann distribution generated with purely local effects (in this case using the SDE) by throwing away the self-intersecting conformations.

The drawback of the SDE approach is that a very large number of sample paths may be required due to the high dimensions of the space (G is six dimensional) and the fact that for chains with finite thickness, a very large percentage of the sample paths can have self-intersections. In the next section, a method for perturbing $f(g;0,L)$ so as to approximate the effects of removing self-intersections from the ensemble *without sampling* is formulated.

4. Statistics of conformational bundles

Let the frame density $f(g;s_1,s_2)$ describe the frequency of occurrence of positions and orientations visited by a frame of reference attached at arc length $s = s_2$ along the backbone curve of a semi-flexible polymer relative to $s = s_1$. The value 0 denotes the proximal end of the chain, and $s = L$ the distal end. If a chain is uniform and short enough for excluded volume to not be important, then $f(g;s_1,s_2) = f(g;0,s_2 - s_1)$. However, for longer chains this will not be true even if they are uniform, because the downstream statistics are not independent of what occurs at the proximal end.

Now imagine that frames of reference are attached at every point on the polymer backbone curve from $s = 0$ to s_1, and all conformations of the polymer are visited with a frequency dictated by Boltzmann statistics. Let us then categorize the distribution of all of these frames of reference according to their starting point (taken as the identity rigid-body motion) and terminating at a particular $g_1 \in G$. Let us call this $m(g_1,g;0,s_1)$, which is illustrated in Fig. 1(b). Here the dependence on $g \in G$ reflects the fact that for fixed g_1 and given $0,s_1$, this will be a distribution of frames of reference. Now suppose that at each frame of reference along the backbone is affixed a rigid body (e.g., base pairs in the case of DNA). In each local reference frame, this body will have a volume described by $p(\mathbf{x})$. The corresponding volume for the whole "bundle of conformations" will be

$$\mu(g_1,\mathbf{x};0,s_1) = \int_G m(g_1,g;0,s_1)p(g^{-1}\cdot\mathbf{x})\,\mathrm{d}g. \tag{11}$$

The function $\mu(g_1,\mathbf{x};0,s_1)$ is the total volume of the ensemble of all configurations which grow from the identity frame fixed to the proximal end of the chain and terminate at the relative frame g_1 for a polymer segment of length s_1.

In an analogous way, it is not difficult to see that integrating the $\mathbf{x}$-dependence out of μ provides the total "volume fraction"[2] occupied by configurations of the chain starting at frame e (at the proximal end) and terminating at frame g_1 (at the distal end). If each residue (or base pair) has volume (i.e., constant volume per unit of arc length of polymer) defined by $\int_{\mathbb{R}^3} p(\mathbf{x})\,\mathrm{d}\mathbf{x}$, this means that the frame density $f(g_1;0,s_1)$ is related to $m(g_1,g;0,s_1)$ and $\mu(g_1,\mathbf{x};0,s_1)$ as

$$f(g_1;0,s_1) = \frac{1}{s_1}\int_G m(g_1,g;0,s_1)\,\mathrm{d}g = \frac{1}{vol(s_1)}\int_{\mathbb{R}^3}\mu(g_1,\mathbf{x};0,s_1)\,\mathrm{d}\mathbf{x}, \tag{12}$$

where $vol(s) = s\cdot\int_{\mathbb{R}^3} p(\mathbf{x})\,\mathrm{d}\mathbf{x}$ is the total volume occupied by one conformation of the homogeneous segment of length s. In the case of a heteropolymer where effectively $p = p(\mathbf{x},s)$, this formulation can be modified slightly, as will be shown later in this paper. Regardless of whether p depends on s or not, when calculating $vol(s)$ it is important that consistent units are used. If s is measured in terms of the number of persistence lengths, the p will be the volume per persistence lengths. If s represents the number of base pairs, then p will be the volume of a single base pair (including the sugar backbone atoms). If s is measured in a unit of length such as nanometers, then p will be measured in volume of backbone per unit length. Whichever unit of length used in the definition of s must be consistent with the units of stiffness used in the definition of $K(s)$. In the current context, s is taken to be measured in units of bending persistence length. Therefore, $s = 1$ corresponds to approximately 150 base pairs.

4.1. Composition formulas

Suppose that s_1 and $s_2 - s_1$ are relatively small segment lengths. In this case, the segments $[0,s_1]$ and $[s_1,s_2]$ will have independent

[2] By this we mean the volume of all conformations with these end constraints normalized by the total number of conformations.

statistics and so we can compute

$$f(g;0,s_2)=\int_G f(h;0,s_1)f(h^{-1}\circ g;s_1,s_2)\,\mathrm{d}h. \tag{13}$$

In these expressions $h\in G$ is a dummy variable of integration. The meaning of (13) is that the distribution of frames of reference at the terminal end of the concatenation of segments is the *group-theoretic convolution* of the frame densities of the terminal ends of each of the two segments relative to their respective bases. With this in mind, the following shorthand notation for (13) is useful:

$$f_{0,s_2}(g)=(f_{0,s_1}*f_{s_1,s_2})(g).$$

A more detailed explanation of why the convolution of frame densities generates the density of the concatenation of segments can be found in the author's previous work [38–42].

Later in the paper the effects of interaction between sequentially distal segments of semi-flexible chains are approximated by considering how the functions $\mu(g,\mathbf{x};0,s_1)$ and $\mu(g,\mathbf{x};s_1,s_2)$ interact. We first note that when the segment $[0,s_2]$ is short, there will be few or no interactions between the subsegments $[0,s_1]$ and $[s_1,s_2]$ due to the semi-flexible nature of the chain. Therefore,

$$\begin{aligned}m(g_1,g;0,s_2)=\int_G &(m(h,g;0,s_1)f(h^{-1}\circ g_1;s_1,s_2)\\ &+f(h;0,s_1)m(h^{-1}\circ g_1,h^{-1}\circ g;s_1,s_2))\,\mathrm{d}h.\end{aligned} \tag{14}$$

This equation says that there are two contributions to $m(g_1,g;0,s_2)$. The first comes from adding up all the contributions due to each $m(h,g;0,s_1)$ for all $h\in G$. This is weighted by the number of upper segment conformations with distal ends that reach the frame g_1 given that their base is at frame h. The second comes from adding up all shifted (translated and rotated) copies of $m(g_1,g;s_1,s_2)$, where the shifting is performed by the lower distribution, and the sum is weighted by the number of distinct configurations of the lower segment that terminate at h. This number is $f(h;0,s_1)\,\mathrm{d}h$.

The veracity of this derivation may be confirmed by integrating the resulting function $m(g_1,g;0,s_2)$ over all values of $g\in G$ and comparing with Eq. (13).

4.2. Generating m from f

In the previous subsection, formulas relating f and μ and their composition were explained. These formulas are true and useful for phantom polymer models in general, though the initial generation of $\mu(g,\mathbf{x};0,s_1)$ for use in (14) by sampling methods can be a problem for continuum models of semi-flexible chains. However, it is possible to directly generate $\mu(\cdot)$ and $m(\cdot)$ if we know $f(g;0,\sigma)$ for all values of $\sigma\in[0,s]$. In particular

$$m(g,h;0,s)=\int_0^s f(h;0,\sigma)f(h^{-1}\circ g;\sigma,s)\,\mathrm{d}\sigma, \tag{15}$$

or more generally,

$$m(g,h;s_1,s_2)=\int_{s_1}^{s_2} f(h;s_1,\sigma)f(h^{-1}\circ g;\sigma,s_2)\,\mathrm{d}\sigma. \tag{16}$$

In other words, the frames of reference that $f(h;0,\sigma)$ contributes to $m(g,h;0,s)$ must be weighted by the probability density of the distal end actually reaching the frame of reference g. This weighting is $f(h^{-1}\circ g;\sigma,s)$. Integration over all values of arc length provides contributions from the full set of frame densities. From (15) and (10) it is clear that

$$\int_G\int_G m(g,h;0,s)\,\mathrm{d}g\,\mathrm{d}h=s_1.$$

Of course, knowing m, one can compute μ from (11), or now include arc length dependence of p as

$$\mu(g,\mathbf{x};0,s)=\int_G\int_0^s f(h;0,\sigma)f(h^{-1}\circ g;\sigma,s)p(h^{-1}\cdot\mathbf{x},\sigma)\,\mathrm{d}\sigma\,\mathrm{d}h. \tag{17}$$

In this general context of non-uniform chains, the volume of the chain defined by the interval $[0,s]$ is

$$vol(s)=\int_0^s\int_{\mathbb{R}^3} p(\mathbf{x},\sigma)\,\mathrm{d}\mathbf{x}\,\mathrm{d}\sigma.$$

It is easy to see by direct integration that

$$\int_{\mathbb{R}^3}\mu(g,\mathbf{x};0,s)\,\mathrm{d}\mathbf{x}=vol(s)\cdot f(g;0,s),$$

which is consistent with (12).

In summary, if the function $f(h;0,\sigma)$ is obtained for all (or finely sampled) values in the range $[0,s]$ by solving (7), then $\mu(g,\mathbf{x};0,s)$ can be obtained in a relatively straightforward manner. This is important, because it will be used for approximating the effects of excluded volume in the next section.

5. Computing averaged effects of excluded volume

The volume of overlap of all conformations contained in the concatenation of two bundles joined at the frame g_1 is

$$n(g_1,g_2;s_1,s_2)=\int_{\mathbb{R}^3}\mu(g_1,\mathbf{x};0,s_1)\mu(g_1^{-1}\circ g_2,g_1^{-1}\cdot\mathbf{x};s_1,s_2)\,\mathrm{d}\mathbf{x}, \tag{18}$$

as illustrated in Fig. 2.

It is important to note that: (1) this cannot distinguish between multiple intersections between two conformations and single intersections between multiple pairs of conformations from the two concatenated bundles; (2) the contribution of each partial overlap is not weighted as heavily in (18) as full overlaps of conformations. Issue (1) is not a concern for semi-flexible chains on the order of a couple of persistence lengths because multiple intersections within a conformation are not likely. We therefore can assume that the major contribution to (18) is due to pairs of conformations from the lower and upper bundles that intersect each other only once. On the other

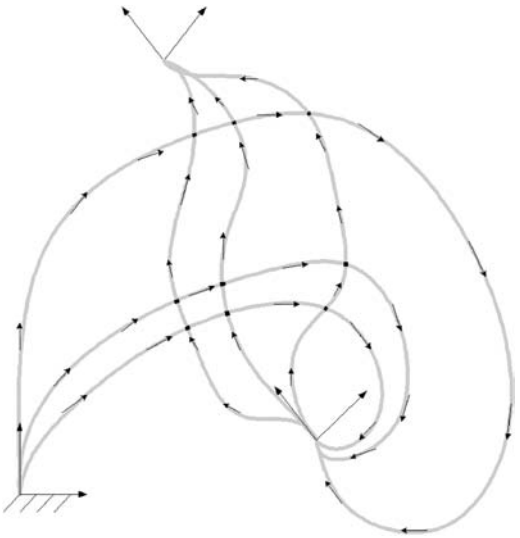

Fig. 2. Approximating excluded-volume interactions using $\mu(g,\mathbf{x})$: two bundles are concatenated and joined at an intermediate reference frame. The intersections of conformations in the two bundles are then counted by Eq. (18). Here arrows along each fiber denote increasing value of arc length.

hand, issue (2) cannot be avoided. The way that it is addressed is to normalize the result of (18) by an estimate of the average volume of overlap that is observed for each possible way that two conformations can intersect.

Computing (18) directly would be computationally intensive, because a three-dimensional integration would have to be performed for each value of the 14 arguments of $n(\cdot)$, i.e., six for each of g_1 and g_2 and one for each s_i, $i=1,2$. Fortunately, the observations about the structure of $\mu(\cdot)$ can be used to reduce the problem to something that is manageable.

Substituting (17) into (18) results in

$$\begin{aligned} n(g_1,g_2;s_1,s_2) &= \int_0^{s_1}\int_{s_1}^{s_2}\int_G\int_G \{f(h_1;0,\sigma_1)f(h_1^{-1}\circ g_1;\sigma_1,s_1)f(h_2;s_1,\sigma_2) \\ &\quad \times f(h_2^{-1}\circ g_1^{-1}\circ g_2;\sigma_2,s_2) \\ &\quad \times v(h_1^{-1}\circ g_1\circ h_2;\sigma_1,\sigma_2)\}\,\mathrm{d}h_1\,\mathrm{d}h_2\,\mathrm{d}\sigma_2\,\mathrm{d}\sigma_1, \end{aligned} \tag{19}$$

where

$$v(g;\sigma_1,\sigma_2)=\int_{\mathbb{R}^3} p(\mathbf{x},\sigma_1)p(g^{-1}\cdot\mathbf{x},\sigma_2)\,\mathrm{d}\mathbf{x}.$$

Note that the change of variables $\mathbf{y}=g^{-1}\cdot\mathbf{x}$ gives

$$\begin{aligned} v(g;\sigma_1,\sigma_2) &= \int_{\mathbb{R}^3} p(g\cdot\mathbf{y},\sigma_1)p(\mathbf{y},\sigma_2)\,\mathrm{d}\mathbf{y} \\ &= \int_{\mathbb{R}^3} p(\mathbf{y},\sigma_2)p(g\cdot\mathbf{y},\sigma_1)\,\mathrm{d}\mathbf{y} = v(g^{-1};\sigma_2,\sigma_1). \end{aligned} \tag{20}$$

Later it will be shown that the following quantity is useful in describing excluded-volume effects:

$$v_0(\sigma_1,\sigma_2)=\int_G v(g;\sigma_1,\sigma_2)\,\mathrm{d}g. \tag{21}$$

5.1. The amount of excluded volume as a function of segment length

While (19) may appear to be hopelessly complicated, in some cases of practical interest, reductions can be made. This is illustrated in the next section. But before doing this, it is worth noting that even while retaining generality, the expression for the quantity

$$N(s_1,s_2)=\int_G\int_G n(g_1,g_2;s_1,s_2)\,\mathrm{d}g_1\,\mathrm{d}g_2$$

can be simplified substantially. This is useful because, for example, plotting the function $q(L)=N(L,2L)$ indicates the total effect that excluded volume has on the density of end-to-end pose.

Returning to (19), if we first integrate over g_2, the result is

$$\begin{aligned} \int_G n(g_1,g_2;s_1,s_2)\,\mathrm{d}g_2 = \int_0^{s_1}\int_{s_1}^{s_2}\int_G\int_G \{&f(h_1;0,\sigma_1) \\ &\times f(h_1^{-1}\circ g_1;\sigma_1,s_1)f(h_2;s_1,\sigma_2) \\ &\times v(h_1^{-1}\circ g_1\circ h_2;\sigma_1,\sigma_2)\}\,\mathrm{d}h_1\,\mathrm{d}h_2\,\mathrm{d}\sigma_2\,\mathrm{d}\sigma_1 \end{aligned}$$

because $f(g;\sigma_2,s_2)$ is a pdf, and integration on G is invariant under left and right shifts (see Appendix A for further explanation).

Now integrating over g_1, and switching the order of integration over h_1,h_2 and g_1 so that the g_1 integral is the innermost one, the following simplification can be made:

$$\begin{aligned} &\int_G f(h_1^{-1}\circ g_1;\sigma_1,s_1)v(h_1^{-1}\circ g_1\circ h_2;\sigma_1,\sigma_2)\,\mathrm{d}g_1 \\ &\quad = \int_G f(k;\sigma_1,s_1)v(k\circ h_2;\sigma_1,\sigma_2)\,\mathrm{d}k, \end{aligned}$$

where the change of variables $k=h_1^{-1}\circ g_1$ is employed. If we apply the symmetry in (20) and use (31), it is clear that the above integrals can be written as

$$\int_G v(h_2^{-1}\circ k^{-1};\sigma_2,\sigma_1)f(k;\sigma_1,s_1)\,\mathrm{d}k=(v_{\sigma_2,\sigma_1}*f_{\sigma_1,s_1})(h_2^{-1}).$$

Then we have

$$\begin{aligned} N(s_1,s_2)=\int_0^{s_1}\int_{s_1}^{s_2}\int_G\int_G &f(h_1;0,\sigma_1) \\ &\times f(h_2;s_1,\sigma_2)(v_{\sigma_2,\sigma_1}*f_{\sigma_1,s_1})(h_2^{-1})\,\mathrm{d}h_1\,\mathrm{d}h_2. \end{aligned}$$

But these integrals are independent, and so integrating the pdf $f(h_1;0,\sigma_1)$ over $\mathrm{d}h_1$ produces 1. Hence

$$N(s_1,s_2)=\int_0^{s_1}\int_{s_1}^{s_2}\int_G f(h_2;s_1,\sigma_2)(v_{\sigma_2,\sigma_1}*f_{\sigma_1,s_1})(h_2^{-1})\,\mathrm{d}h_1\,\mathrm{d}h_2.$$

This can be written in the compact notation

$$\begin{aligned} N(s_1,s_2) &= \int_0^{s_1}\int_{s_1}^{s_2}(v_{\sigma_2,\sigma_1}*f_{\sigma_1,s_1}*f_{s_1,\sigma_2})(e)\,\mathrm{d}\sigma_2\,\mathrm{d}\sigma_1 \\ &= \int_0^{s_1}\int_{s_1}^{s_2}(v_{\sigma_2,\sigma_1}*f_{\sigma_1,\sigma_2})(e)\,\mathrm{d}\sigma_2\,\mathrm{d}\sigma_1. \end{aligned} \tag{22}$$

The above equation is easy to evaluate and provides a means to determine how the effects of excluded volume change with segment length.

5.2. Approximating the end-pose distribution for conformations with excluded volume

If we desire to determine how excluded volume changes the distribution of end-to-end positions and orientations (or end-to-end distance), then we seek to compute

$$\begin{aligned} n'(g_2;s_1,s_2) &= \int_G n(g_1,g_2;s_1,s_2)\,\mathrm{d}g_1 \\ &= \int_0^{s_1}\int_{s_1}^{s_2}\int_G\int_G f(h_1;0,\sigma_1)f(k;\sigma_1,\sigma_2) \\ &\quad \times f(k^{-1}\circ h_1^{-1}\circ g_2;\sigma_2,s_2)v(k;\sigma_1,\sigma_2)\,\mathrm{d}k\,\mathrm{d}h_1\,\mathrm{d}\sigma_2\,\mathrm{d}\sigma_1 \\ &= \int_0^{s_1}\int_{s_1}^{s_2}(f_{0,\sigma_1}*(v\cdot f)_{\sigma_1,\sigma_2}*f_{\sigma_2,s_2})(g_2)\,\mathrm{d}\sigma_2\,\mathrm{d}\sigma_1. \end{aligned} \tag{23}$$

Here the change of variables $k=h_1^{-1}\circ g_1\circ h_2$ is used together with the definition of convolution (several times). The notation $(v\cdot f)(g)$ simply means point-wise multiplication, i.e., $(v\cdot f)(g)=v(g)f(g)$, which is the scalar multiplication of $v(g)$ and $f(g)$ at each value of $g\in G$.

In the general case, (23) does not simplify further, though even in the general case methods developed previously by the author in principle can be used to compute such convolutions efficiently [40,91]. However, as will be seen in the specific examples that follow, simplifications result from symmetries in f and the nature of v.

Assuming that $n'(g_2;s_1,s_2)$ can be computed, the effects of excluded volume are incorporated into the pose distribution by subtracting from the result that would be obtained from the phantom model:

$$f'(g;0,s_2)=f(g;0,s_2)-n'(g;s_1,s_2)/\overline{V}_\cap(s_2). \tag{24}$$

$f(g;0,s_2)$ can be obtained by either solving the diffusion equation up to length s_2, or by convolving $f(g;0,s_1)$ and $f(g;s_1,s_2)$. Here we normalize by $\overline{V}_\cap(s_2)$, which is the average volume of intersection of each chain from the lower bundle of conformations with each chain from the upper one. We are assuming that this is independent of g_2. The average is taken over all possible ways that two chains

can intersect. For example, they can intersect dead on at any angle, or they can intersect very slightly due to paths that meet almost tangentially. Then we can compute

$$f''(g;0,s_2)=f'(g;0,s_2)\Big/\int_G f'(g;0,s_2)\,\mathrm{d}g \tag{25}$$

which ensures that the result is a pdf. This can be done for different estimates of $\overline{V}_\cap(s_2)$ to examine the range of effects that excluded volume can have on the end-pose distribution. Eq. (25) can be viewed as a perturbation of f that approximates excluded-volume effects.

6. Numerical and analytical results

In the general case, v has no symmetries and (23) cannot be simplified further. However, there are wide classes of v's that have symmetries compatible with those of f that will reduce (23) to a simpler form. For example, if the cross-sectional dimensions of a polymer are small relative to its length, and each $p(\mathbf{x},\sigma_i)$ is axially symmetric around the x_3-axis, then effectively

$$v(g;\sigma_1,\sigma_2)=\frac{v_0(\sigma_1,\sigma_2)}{2\pi}\int_0^{2\pi}\delta(r_3(-\theta)\circ g)\,\mathrm{d}\theta,$$

where $r_3(\theta)$ denotes pure rotation around the x_3-axis and v_0 is defined in (21). If $f(g)=f(r_3(\theta)\circ g)$ for all $\theta\in[0,2\pi]$ (i.e., the distribution at the distal end is invariant under rotations of the proximal end) then the middle equation in (23) reduces to

$$n'(g_2;s_1,s_2)=\int_0^{s_1}\int_{s_1}^{s_2}v_0(\sigma_1,\sigma_2)f_{\sigma_1,\sigma_2}(e)\cdot(f_{0,\sigma_1}*f_{\sigma_2,s_2})(g_2)\,\mathrm{d}\sigma_2\,\mathrm{d}\sigma_1. \tag{26}$$

This follows from the definition of convolution on G, changing the order of integrations, and the axial symmetry of $f(g)$:

$$\begin{aligned}
&((v\cdot f)_{\sigma_1,\sigma_2}*f_{\sigma_2,s_2})(g)\\
&=\int_G(v\cdot f)_{\sigma_1,\sigma_2}(h)f_{\sigma_2,s_2}(h^{-1}\circ g)\,\mathrm{d}h\\
&=\frac{v_0(\sigma_1,\sigma_2)}{2\pi}\int_0^{2\pi}\left[\int_G\delta(r_3(-\theta)\circ h)f_{\sigma_1,\sigma_2}(h)f_{\sigma_2,s_2}(h^{-1}\circ g)\,\mathrm{d}h\right]\mathrm{d}\theta\\
&=\frac{v_0(\sigma_1,\sigma_2)}{2\pi}\int_0^{2\pi}f_{\sigma_1,\sigma_2}(r_3(\theta))f_{\sigma_2,s_2}(r_3(-\theta)\circ g)\,\mathrm{d}\theta\\
&=\frac{v_0(\sigma_1,\sigma_2)}{2\pi}\int_0^{2\pi}f_{\sigma_1,\sigma_2}(e)f_{\sigma_2,s_2}(g)\,\mathrm{d}\theta\\
&=v_0(\sigma_1,\sigma_2)f_{\sigma_1,\sigma_2}(e)f_{\sigma_2,s_2}(g).
\end{aligned}$$

Substituting this in (23) results in (26).

Similarly, if the cross-sectional density is assumed to be concentrated in position, but isotropic in orientation, such as $v((R,\mathbf{r});\sigma_1,\sigma_2)=(v_0(\sigma_1,\sigma_2)/8\pi^2)\delta(\mathbf{r})$, and if f is assumed to be isotropic in orientation, then the same simplified expression for $n'(g_2;s_1,s_2)$ results.

If the chain is uniform $f_{s_1,s_2}=f_{0,s_2-s_1}$, $v_0(\sigma_1,\sigma_2)=v_0$ is constant, and (26) reduces to

$$\begin{aligned}
n'(g_2;s_1,s_2)&=v_0\int_0^{s_1}\int_{s_1}^{s_2}f_{0,\sigma_2-\sigma_1}(e)\cdot f_{0,s_2-\sigma_2+\sigma_1}(g_2)\,\mathrm{d}\sigma_2\,\mathrm{d}\sigma_1\\
&=v_0\int_0^{s_2}w(s;s_1,s_2)\cdot f_{0,s}(e)\cdot f_{0,s_2-s}(g_2)\,\mathrm{d}s,
\end{aligned}$$

where $w(s;s_1,s_2)$ is a factor resulting from integration by parts (see Appendix A). The benefit of writing it in this way is a reduction in the number of arithmetic operations that need to be performed when computing the integral numerically. In the uniform case, (22) can be written immediately by integrating n' over g_2 as

$$N(s_1,s_2)=v_0\int_0^{s_2}w(s;s_1,s_2)\cdot f_{0,s}(e)\,\mathrm{d}s.$$

Similarly, in the uniform case, $v_0=\varepsilon\overline{V}_\cap$ for some $\varepsilon\in[0,1]$, and so

$$f'_{0,s_2}(g)=f_{0,s_2}(g)-\varepsilon\int_0^{s_2}w(s;s_1,s_2)\cdot f_{0,s}(e)\cdot f_{0,s_2-s}(g)\,\mathrm{d}s.$$

If we view the positional part of $g=(R,\mathbf{r})$ as being parameterized in spherical coordinates so that $\mathbf{r}=r\mathbf{u}(\phi,\theta)$, then the end-to-end distance distribution corresponding to f' will be

$$f'_{0,s_2}(r)=r^2\int_{SO(3)}\int_{S^2}f'_{0,s_2}(g)\,\mathrm{d}\mathbf{u}\,\mathrm{d}R,$$

where S^2 is the unit sphere and $\mathrm{d}\mathbf{u}=\sin\theta\,\mathrm{d}\phi\,\mathrm{d}\theta$. Since these integrals commute with the integral over s, it means that

$$f'_{0,s_2}(r)=f_{0,s_2}(r)-\varepsilon\int_0^{s_2}w(s;s_1,s_2)\cdot f_{0,s}(e)\cdot f_{0,s_2-s}(r)\,\mathrm{d}s.$$

In other words, if we only want to compute $f''_{0,s_2}(r)$, then we can do so by using the end-to-end distance distributions $f_{0,s_2-s}(r)$ and the J factor, $f_{0,s}(e)$, to compute $f'_{0,s_2}(r)$, and then normalize the result to be a pdf in the radial variable, r.

For the Kratky–Porod worm-like chain, $D_{11}=D_{22}=2L$ where L is the number of persistence lengths of the chain. The functions $f_{0,L}(r)$ and $f_{0,L}(e)$ can be computed for various values of L using the second-order Daniels approximation [1,37]:

$$f^D_{0,L}(r)=4\pi r^2\Phi(r,L)\left(\frac{3}{2\pi L}\right)^{3/2}\exp\left(-\frac{3r^2}{2L}\right)\quad\text{and}$$

$$f^D_{0,L}(e)=\left(\frac{3}{2\pi L}\right)^{3/2}\Phi(0,L),$$

where

$$\begin{aligned}
\Phi(r,L)=1&-\frac{5}{8L}+\frac{2r^2}{L^2}-\frac{33r^4}{40L^3}-\frac{79}{640L^2}-\frac{329r^2}{240L^3}+\frac{6799r^4}{1600L^4}\\
&-\frac{3441r^6}{1400L^5}+\frac{1089r^8}{3200L^6}.
\end{aligned}$$

This is an asymptotic expansion of a phantom semi-flexible chain that becomes more accurate as L becomes large (i.e., when the chain consists of multiple persistence lengths, $L\gg1$). When $L\leqslant1$, the Daniels approximation can become negative at some values of r. When $L\ll1$, the J factor becomes zero, and the distribution of end-to-end distances becomes a Dirac delta function. Combining these facts, we have

$$f_{0,L}(r)=\begin{cases}f^D_{0,L}(r) & \text{for } L>2,\\ \max\{f^D_{0,L}(r),0\}\Big/\displaystyle\int_0^1\max\{f^D_{0,L}(r'),0\}\,\mathrm{d}r' & \text{for } L\in[1/2,2],\\ \delta(r-L) & \text{for } L\in[0,1/2]\end{cases}$$

and

$$f_{0,L}(e)=\begin{cases}f^D_{0,L}(e) & \text{for } L>0.7827,\\ 0 & \text{for } L\leqslant0.7827.\end{cases}$$

Note that $L=0.7827$ is the crossing point where $\Phi(0,L)$ becomes zero, and for values of L smaller than this, $\Phi(0,L)$ is always negative.

As an alternative, it is possible to solve (7) for the KP model using techniques from Noncommutative Harmonic Analysis as was done in [38,40].

Fig. 3 compares end-to-end probability density estimates obtained from sample paths of the stochastic elastica for the KP chain

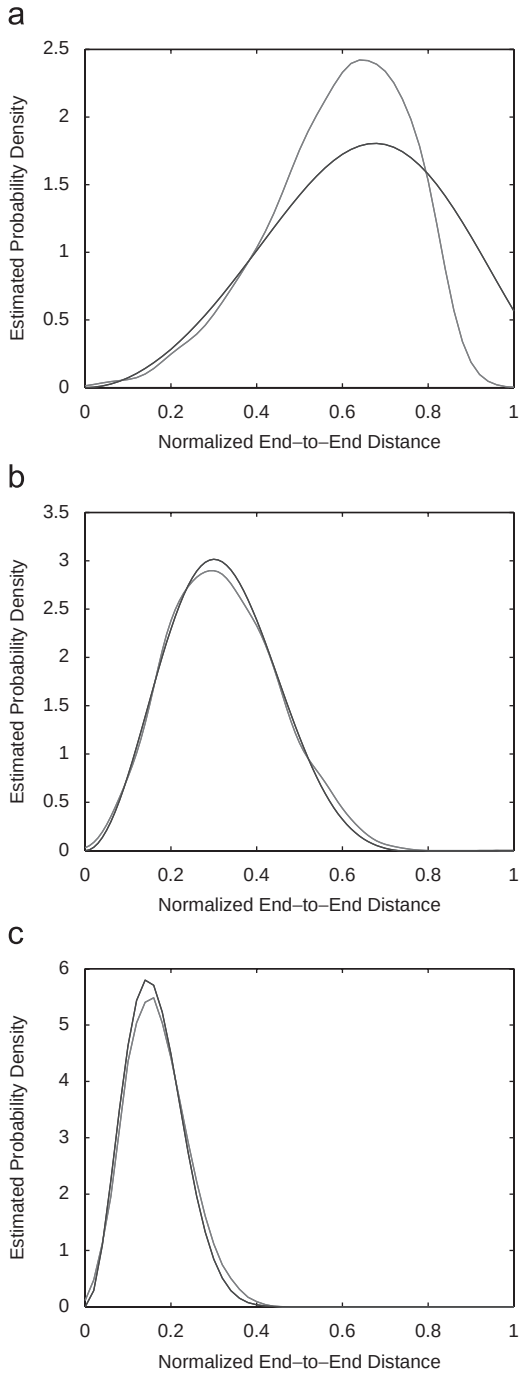

Fig. 3. Comparison of the clipped second-order Daniels approximation (blue) with density estimate constructed from 1000 sample paths of the stochastic elastica (red) for different values of diffusion parameter. Red density is reconstructed using Gaussian Kernels with optimal smoothing parameter. Recall that the strength of the noise term in the SDE has a standard deviation of $\sqrt{D_{11}}$ when the bending persistence length is $L=D_{11}$. (a) Diffusion parameter $\sqrt{D_{11}}=2$. (b) Diffusion parameter $\sqrt{D_{11}}=4$. (c) Diffusion parameter $\sqrt{D_{11}}=8$. (For interpretation of the references to color in this figure legend, the reader is referred to the web version of this article).

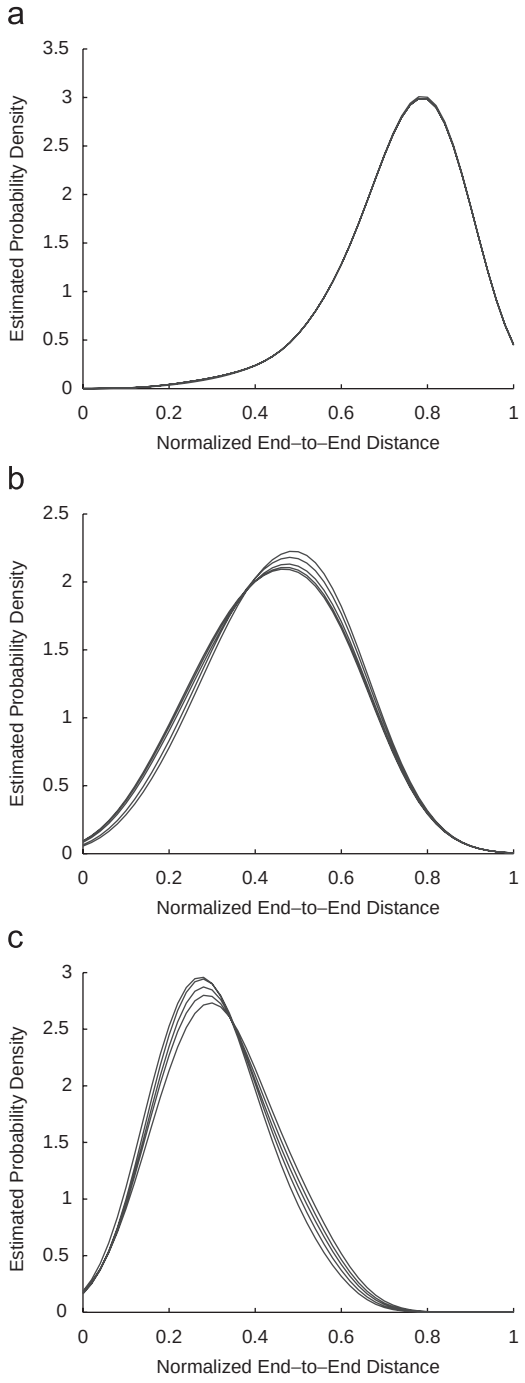

Fig. 4. The significance of excluded volume as a function of chain length. In each plot, end-to-end distances are shown for self-avoiding conformations with radii (measured in units of persistence length) ranging over a factor of five. Even for very thick chains and many persistence lengths the effects are small. (a) Persistence length = 1, chain radius ranging from 0.02 to 0.1. (b) Persistence length=4, chain radius ranging from 0.02 to 0.1. (c) Persistence length = 10, chain radius ranging from 0.02 to 0.1.

with the clipped and normalized Daniels approximation, $f_{0,L}(r)$, where L is the number of persistence lengths. In the plot, lengths are normalized to the length of the polymer. As can be seen, the Daniels approximation breaks down for small values of L.

Sample paths of the stochastic elastica are generated using the Euler–Maruyama algorithm described in [92] applied to (4). In this method each dW_i is independently sampled at each time step from a Gaussian distribution with unit variance. The author of [92] has posted such code on the web. The resulting $\xi(k\Delta s)$ for $k=1,\ldots,L/\Delta s$ is then "injected" from the Lie algebra to the Lie group G by computing the following product of exponentials [93]:

$$g(n\Delta s)=\exp(\Delta s\hat{\xi}(\Delta s))\exp(\Delta s\hat{\xi}(2\Delta s))\cdots\exp(\Delta s\hat{\xi}(n\Delta s)), \tag{27}$$

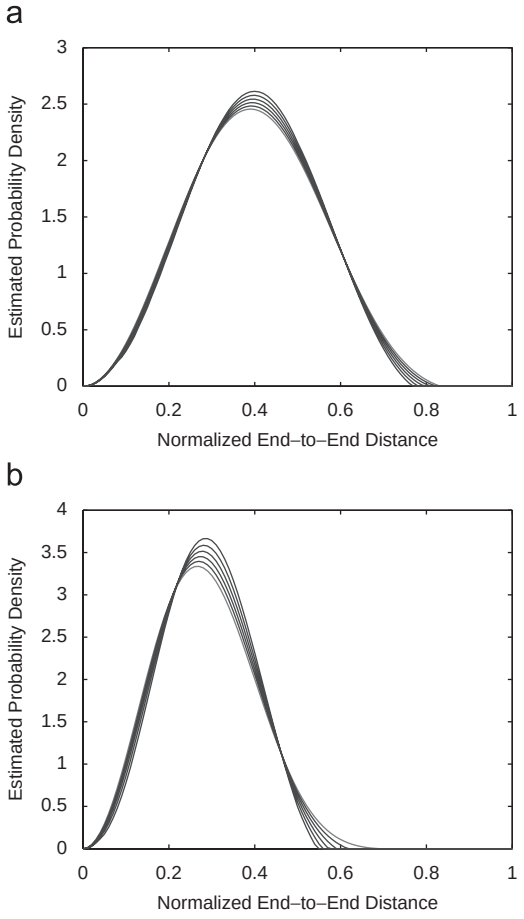

Fig. 5. End-to-end distance distribution for a semi-flexible chain with excluded volume computed using the conformational bundle approach. Daniels in red. Excluded-volume perturbations to Daniels in blue (a) Input persistence length $L=2.5$, parameter ε ranging from 0.05 to 0.25. (b) Input persistence length $L=5$, parameter ε ranging from 0.05 to 0.25. (For interpretation of the references to color in this figure legend, the reader is referred to the web version of this article).

which approximates the product integral described in [82]. Each sample path is then tested to determine whether or not any two positions along the path are too close to each other (i.e., within $2r$ of each other, where r is the radius of the cross-section). Those that are close are removed. Fig. 4 illustrates the relative importance of excluded volume as a function of persistence length. If the persistence length is less than 1, the end-to-end distributions are not influenced by excluded-volume effects. As the persistence length increases, so too do the excluded-volume effects. However, their influence on the end-to-end distance distribution are quite modest. In Fig. 4(a), a thick chain one persistence-length long has only one self-intersection out of 500 sample paths when the radius is 0.1 persistence lengths. DNA has a thickness far less than this. In Fig. 4(b), 1000 sample paths of a chain consisting of four persistence lengths are generated for chain radii ranging from 0.02 to 0.1 persistence lengths. Of these, 990, 977, 959, 920, and 886 survive without self-interpenetration. In Fig. 4(c), 500 sample paths of a chain of length 10 persistence lengths are generated for chain radii ranging from 0.02 to 0.1. Of these, 496, 476, 436, 411, and 385 survive without self-interpenetration.

Fig. 5 shows the pdf of end-to-end distance with excluded-volume effects incorporated for chains of different values of ε for each L using the conformational-bundle approach in Eq. (25) when using the clipped and normalized Daniels approximation as the input. As can be seen, the effects of excluded volume become more important as the chain length and ε increase, but again, they are quite modest. Furthermore, the results are similar in that excluded-volume effect has a tendency to push the mode of the pdf towards the right side. This becomes more pronounced as the radius of the chain is increased.

7. Conclusions

A new model for computing the effects of excluded volume in semi-flexible polymer statistical mechanics has been presented. This models take as its input the probability densities describing the frequency of occurrence of frames of reference attached at points on the backbone curve of short phantom polymer segments. For short uniform segments, this pose distribution can be obtained by solving a diffusion equation. The SDE corresponding to this diffusion equation is used to generate longer chains, where the excluded-volume effect cannot be ignored. Self-intersecting conformations are removed from the ensemble and statistical quantities of interest are calculated. A theory for obtaining the density corresponding to a bundle of conformations is presented. The overlap of conformational bundles between adjacent segments is used to estimate the effects of excluded volume between them. Numerical results quantify the magnitude of the excluded-volume effect and show that this method generates comparable results as the brute-force SDE approach, but at a lower computational cost.

Acknowledgments

This work was performed under support from the NIH Grant R01 GM075310 “Group Theoretic Methods in Protein Structure Determination.” Thanks go to Ms. Yingyu Wang for producing Figs. 1 and 2.

Appendix A

A.1. Explicit form of Lie derivatives for the Euclidean motion group

It can be shown that for $G=E(3)$, [38–40]

$$\tilde{X}_i^r = \begin{cases} X_i^r & \text{for } i=1,2,3, \\ (R^{\mathrm{T}}\nabla_{\mathbf{r}})_{i-3} & \text{for } i=4,5,6 \end{cases} \tag{28}$$

and

$$\tilde{X}_i^l = \begin{cases} X_i^l + \sum_{k=1}^{3} (\mathbf{r}\times\mathbf{e}_i)\cdot\mathbf{e}_k \dfrac{\partial}{\partial r_k} & \text{for } i=1,2,3, \\ -\dfrac{\partial}{\partial r_{i-3}} & \text{for } i=4,5,6. \end{cases} \tag{29}$$

Here $\nabla_q f=[\partial f/\partial q_1, \partial f/\partial q_2, \partial f/\partial q_3]^{\mathrm{T}}$ and $X_i^r f=(\nabla_q f)\cdot(J_r^{-1}\mathbf{e}_i)$ is the $SO(3)$ differential operator with J_r being the Jacobian that relates angular velocity as seen in the moving frame to the rate of change of the rotational parameterization q as $\boldsymbol{\omega}_r = J_r\dot{\mathbf{q}}$. An analogous relationship holds for the left operators and angular velocity as observed from the inertial reference frame.

For example, if R is parameterized with ZXZ Euler angles so that $R=R(\alpha,\beta,\gamma)$, then the X_i^r are defined as

$$\begin{aligned} X_1^r &= -\cot\beta\sin\gamma\frac{\partial}{\partial\gamma} + \frac{\sin\gamma}{\sin\beta}\frac{\partial}{\partial\alpha} + \cos\gamma\frac{\partial}{\partial\beta}, \\ X_2^r &= -\cot\beta\cos\gamma\frac{\partial}{\partial\gamma} + \frac{\cos\gamma}{\sin\beta}\frac{\partial}{\partial\alpha} - \sin\gamma\frac{\partial}{\partial\beta}, \\ X_3^r &= \frac{\partial}{\partial\gamma}. \end{aligned} \tag{30}$$

When rotations are parameterized using the ZXZ Euler angles (α,β,γ).

A.2. Integration and convolution on the Euclidean motion group

Any element of $G=E(3)$ can be parameterized as $g=(R(\alpha,\beta,\gamma),\mathbf{r})$ where $R(\alpha,\beta,\gamma)=R_3(\alpha)R_1(\beta)R_3(\gamma)$ are the ZXZ Euler angles, and $\mathbf{r}^{\mathrm{T}}=[r_1,r_2,r_3]^{\mathrm{T}}$ are Cartesian coordinates of the translational part of g. The range of the Euler angles is $0\leqslant\alpha,\ \gamma\leqslant 2\pi$ and $0\leqslant\beta\leqslant\pi$. The volume element for G is given by

$$\mathrm{d}g=\frac{1}{8\pi^2}\sin\beta\,\mathrm{d}\alpha\,\mathrm{d}\beta\,\mathrm{d}\gamma\,\mathrm{d}r_1\,\mathrm{d}r_2\,\mathrm{d}r_3,$$

which is the product of the volume elements for $\mathbb{R}^3$ ($\mathrm{d}\mathbf{r}=\mathrm{d}r_1\,\mathrm{d}r_2\,\mathrm{d}r_3$), and for $SO(3)$ ($\mathrm{d}R=(1/8\pi^2)\sin\beta\,\mathrm{d}\alpha\,\mathrm{d}\beta\,\mathrm{d}\gamma$). The normalization factor in the definition of $\mathrm{d}R$ is so that $\int_{SO(3)}\mathrm{d}R=1$.

We note the following shorthands used throughout the paper:

$$\int_{SO(3)}=\int_0^{2\pi}\int_0^{\pi}\int_0^{2\pi},$$

$$\int_{\mathbb{R}^3}=\int_{r_1=-\infty}^{\infty}\int_{r_2=-\infty}^{\infty}\int_{r_3=-\infty}^{\infty}$$

and

$$\int_G=\int_{\mathbb{R}^3}\int_{SO(3)}.$$

Integration on $G=E(3)$ is invariant under left and right shifts by arbitrary $h\in G$, and inversions i.e.,

$$\int_G f(g)\,\mathrm{d}g=\int_G f(h^{-1}\circ g)\,\mathrm{d}g=\int_G f(g\circ h)\,\mathrm{d}g=\int_G f(g^{-1})\,\mathrm{d}g.$$

This is well known in certain communities (see e.g. [40,90,94]).

A convolution integral of the form

$$(f_1*f_2)(g)=\int_G f_1(h)f_2(h^{-1}\circ g)\,\mathrm{d}h$$

can be written in the following equivalent ways:

$$(f_1*f_2)(g)=\int_G f_1(z^{-1})f_2(z\circ g)\,\mathrm{d}z=\int_G f_1(g\circ k^{-1})f_2(k)\,\mathrm{d}k,\tag{31}$$

where the substitutions $z=h^{-1}$ and $k=h^{-1}\circ g$ have been made, and the invariance of integration under shifts and inversions is used.

A.3. Derivation of $w(s;s_1,s_2)$

Here we prove that for an arbitrary continuous, integrable and bounded function $x(s)$, the following identity holds:

$$\int_0^{s_1}\int_{s_1}^{s_2}x(\sigma_2-\sigma_1)\,\mathrm{d}\sigma_2\,\mathrm{d}\sigma_1=\int_0^{s_2}w(s;s_1,s_2)x(s)\,\mathrm{d}s,\tag{32}$$

where $w(s;s_1,s_2)$ is a function to be determined. Define

$$X(s)=\int_0^{s}x(\sigma)\,\mathrm{d}\sigma.$$

Then, by the change of variables $\sigma=\sigma_2-\sigma_1$, the inner integral on the left side of Eq. (32) becomes

$$\int_{s_1}^{s_2}x(\sigma_2-\sigma_1)\,\mathrm{d}\sigma_2=X(s_2-\sigma_1)-X(s_1-\sigma_1).$$

Now we integrate each of these by parts. The first term becomes

$$\begin{aligned}\int_0^{s_1}X(s_2-\sigma_1)\,\mathrm{d}\sigma_1&=X(s_2-\sigma_1)\sigma_1|_0^{s_1}+\int_0^{s_1}\sigma_1x(s_2-\sigma_1)\,\mathrm{d}\sigma_1\\&=s_1\int_0^{s_2-s_1}x(\sigma)\,\mathrm{d}\sigma+\int_{s_2-s_1}^{s_2}(s_2-\sigma)x(\sigma)\,\mathrm{d}\sigma.\end{aligned}\tag{33}$$

Now performing the following integration by parts:

$$\begin{aligned}\int_0^{s_1}X(s_1-\sigma_1)\,\mathrm{d}\sigma_1&=X(s_1-\sigma_1)\sigma_1|_0^{s_1}+\int_0^{s_1}\sigma_1x(s_1-\sigma_1)\,\mathrm{d}\sigma_1\\&=\int_0^{s_1}(s_1-\sigma)x(\sigma)\,\mathrm{d}\sigma\end{aligned}\tag{34}$$

and subtracting (34) from (33), we see that

$$\begin{aligned}&\int_0^{s_1}\int_{s_1}^{s_2}x(\sigma_2-\sigma_1)\,\mathrm{d}\sigma_2\,\mathrm{d}\sigma_1\\&=s_1\int_0^{s_2-s_1}x(\sigma)\,\mathrm{d}\sigma+\int_{s_2-s_1}^{s_2}(s_2-\sigma)x(\sigma)\,\mathrm{d}\sigma-\int_0^{s_1}(s_1-\sigma)x(\sigma)\,\mathrm{d}\sigma.\end{aligned}$$

This can be written in the form of (32) when

$$\begin{aligned}w(s;s_1,s_2)=&-(s_1-s)W(s,0,s_1)+(s_2-s)W(s,s_2-s_1,s_2)\\&+s_1W(s,0,s_2-s_1),\end{aligned}\tag{35}$$

where $W(s,a,b)$ is the window function that takes the value of 1 on the interval $(a,b]$, and zero otherwise. As a special case, when $s_1=L$ and $s_2=2L$, things simplify to

$$w(s;L,2L)=sW(s,0,L)+(2L-s)W(s,L,2L),$$

which is simply a triangular function with peak value of L at $s=L$ and a value of zero at $s=0$ and $s=2L$.

References

[1] H.E. Daniels, The statistical theory of stiff chains, Proc. R. Soc. (Edinburgh) A63 (1952) 290–311.
[2] J.J. Hermans, R. Ullman, The statistics of stiff chains, with applications to light scattering, Physica 18 (11) (1952) 951–971.
[3] O. Kratky, G. Porod, Röntgenuntersuchung Gelöster Fadenmoleküle, Recl. Trav. Chim. Pays Bas 68 (12) (1949) 1106–1122.
[4] W. Gobush, H. Yamakawa, W.H. Stockmayer, W.S. Magee, Statistical mechanics of wormlike chains. I. Asymptotic behavior, J. Chem. Phys. 57 (7) (1972) 2839–2843.
[5] M. Schmidt, W.H. Stockmayer, Quasi-elastic light scattering by semiflexible chains, Macromolecules 17 (4) (1984) 509–514.
[6] J. Shimada, H. Yamakawa, Statistical mechanics of DNA topoisomers, J. Mol. Biol. 184 (1985) 319–329.
[7] D. Shore, R.L. Baldwin, Energetics of DNA twisting, J. Mol. Biol. 170 (1983) 957–981.
[8] A.V. Vologodskii, V.V. Anshelevich, A.V. Lukashin, M.D. Frank-Kamenetskii, Statistical mechanics of supercoils and the torsional stiffness of the DNA double helix, Nature 280 (1979) 294–298.
[9] H. Yamakawa, W.H. Stockmayer, Statistical mechanics of wormlike chains. II. Excluded volume effects, J. Chem. Phys. 57 (7) (1972) 2843–2854.
[10] P.J. Hagerman, Analysis of the ring-closure probabilities of isotropic wormlike chains: application to duplex DNA, Biopolymers 24 (1985) 1881–1897.
[11] J. Wilhelm, E. Frey, Radial distribution function of semiflexible polymers, Phys. Rev. Lett. 77 (12) (1996) 2581–2584.
[12] B.Y. Ha, D. Thirumalai, Semiflexible chains under tension, J. Chem. Phys. 106 (8) (1997) 4243–4247.
[13] J.B. Lagowski, J. Noolandi, B. Nickel, Stiff chain model—functional integral approach, J. Chem. Phys. 95 (2) (1991) 1266–1269.
[14] T.B. Liverpool, R. Golestanian, K. Kremer, Statistical mechanics of double-stranded semiflexible polymers, Phys. Rev. Lett. 80 (2) (1998) 405–408.
[15] S. Matsutani, Statistical mechanics of no-stretching elastica in three-dimensional space, J. Geom. Phys. 29 (1999) 243–259.
[16] T. Odijk, Stiff chains and filaments under tension, Macromolecules 28 (20) (1995) 7016–7018.
[17] Y. Shi, S. He, J.E. Hearst, Statistical mechanics of the extensible and shearable elastic rod and of DNA, J. Chem. Phys. 105 (2) (1996) 714–731.
[18] S. Stepanow, Kramer equation as a model for semiflexible polymers, Phys. Rev. E 54 (3) (1996) R2209–R2211.
[19] R.G. Winkler, L. Harnau, P. Reineker, Distribution functions and dynamical properties of stiff macromolecules, Macromol. Theory Simul. 6 (1997) 1007–1035.
[20] R.G. Winkler, Analytical calculation of the relaxation dynamics of partially stretched flexible chain molecules: necessity of a wormlike chain description, Phys. Rev. Lett. 82 (9) (1999) 1843–1846.
[21] S.R. Zhao, C.P. Sun, W.X. Zhang, Statistics of wormlike chains. I. Properties of a single chain, J. Chem. Phys. 106 (6) (1997) 2520–2529.

[22] A.L. Kholodenko, Statistical mechanics of semiflexible polymers: yesterday, today and tomorrow, J. Chem. Soc. Faraday Trans. 91 (16) (1995) 2473–2482.
[23] K. Klenin, H. Merlitz, J. Langowski, A Brownian dynamics program for the simulation of linear and circular DNA and other wormlike chain polyelectrolytes, Biophys. J. 74 (1998) 780–788.
[24] K. Kroy, E. Frey, Force-extension relation and plateau modulus for wormlike chains, Phys. Rev. Lett. 77 (2) (1996) 306–309.
[25] M.G. Bawendi, F.F. Karl, A Wiener integral model for stiff polymer chains, J. Chem. Phys. 83 (5) (1985) 2491–2496.
[26] S.M. Bhattacharjee, M. Muthukumar, Statistical mechanics of solutions of semiflexible chains: a Pathe integral formulation, J. Chem. Phys. 86 (1) (1987) 411–418.
[27] T.B. Liverpool, S.F. Edwards, Probability distribution of wormlike polymer loops, J. Chem. Phys. 103 (15) (1995) 6716–6719.
[28] A. Miyake, Stiff-chain statistics in relation to the Brownian process, J. Phys. Soc. Jpn. 50 (5) (1981) 1676–1682.
[29] M. Doi, S.F. Edwards, The Theory of Polymer Dynamics, Clarendon Press, Oxford, 1986.
[30] P.J. Flory, Statistical Mechanics of Chain Molecules, Wiley-Interscience, New York, 1969.
[31] T. Norisuye, A. Tsuboi, A. Teramoto, Remarks on excluded-volume effects in semiflexible polymer solutions, Polym. J. 28 (4) (1996) 357–361.
[32] P.G. de Gennes, Scaling Concepts in Polymer Physics, Cornell University Press, 1979.
[33] L. Shäfer, Excluded Volume Effects in Polymer Solutions, As Explained by the Renormalization Group, Springer, New York, 1999.
[34] D. Thirumalai, B.-Y. Ha, Statistical mechanics of semiflexible chains: a mean field variational approach, in: A. Grosberg (Ed.), Theoretical and Mathematical Models in Polymer Research, Academic Press, New York, 1998, pp. 1–35.
[35] J. des Cloizeaux, G. Jannink, Polymers in Solution: Their Modelling and Structure, Clarendon Press, Oxford, 1990.
[36] A.Yu. Grosberg, A.R. Khokhlov, Statistical Physics of Macromolecules, American Institute of Physics, New York, 1994.
[37] H. Yamakawa, Helical Wormlike Chains in Polymer Solutions, Springer, Berlin, 1997.
[38] G.S. Chirikjian, Y.F. Wang, Conformational statistics of stiff macromolecules as solutions to PDEs on the rotation and motion groups, Phys. Rev. E 62 (1) (2000) 880–892.
[39] G.S. Chirikjian, A.B. Kyatkin, An operational calculus for the Euclidean motion group with applications in robotics and polymer science, J. Fourier Anal. Appl. 6 (6) (2000) 583–606.
[40] G.S. Chirikjian, A.B. Kyatkin, Engineering Applications of Noncommutative Harmonic Analysis, CRC Press, Boca Raton, FL, 2001.
[41] G.S. Chirikjian, Stochastic Models, Information Theory, and Lie Groups, Birkhäuser, 2009.
[42] G.S. Chirikjian, Conformational statistics of macromolecules using generalized convolution, Comput. Theor. Polym. Sci. 11 (2001) 143–153.
[43] C.G. Baumann, S.B. Smith, V.A. Bloomfield, C. Bustamante, Ionic effects on the elasticity of single DNA molecules, Proc. Natl. Acad. Sci. USA 94 (12) (1997) 6185–6190.
[44] D.S. Horowitz, J.C. Wang, Torsional rigidity of DNA and length dependence of the free energy of DNA supercoiling, J. Mol. Biol. 173 (1984) 75–91.
[45] J.D. Moroz, P. Nelson, Torsional directed walks, entropic elasticity, and DNA twist stiffness, Proc. Natl. Acad. Sci. USA 94 (26) (1997) 14418–14422.
[46] J.D. Moroz, P. Nelson, Entropic elasticity of twist-storing polymers, Macromolecules 31 (18) (1998) 6333–6347.
[47] S.B. Smith, L. Finzi, C. Busmante, Direct mechanical measurements of the elasticity of single DNA-molecules by using magnetic beads, Science 258 (1992) 1122–1126.
[48] S.D. Levene, D.M. Crothers, Ring closure probabilities for DNA fragments by Monte Carlo simulation, J. Mol. Biol. 189 (1986) 61–72.
[49] C. Buchiat, M.D. Wang, J.F. Allemand, T. Strick, S.M. Block, V. Croquette, Estimating the persistence length of a worm-like chain molecule from force-extension measurements, Biophys. J. 76 (1999) 409–413.
[50] P. Cluzel, A. Lebrun, H. Christoph, R. Lavery, J.L. Viovy, D. Chatenay, F. Caron, DNA: an extensible molecule, Science 271 (1996) 792.
[51] R.D. Kamein, T.C. Lubensky, P. Nelson, C.S. O'Hern, Direct determination of DNA twist–stretch coupling, Europhys. Lett. 28 (3) (1997) 237–242.
[52] J.F. Marko, E.D. Siggia, Bending and twisting elasticity of DNA, Macromolecules 27 (1994) 981–988.
[53] J.F. Marko, DNA under high tension: overstretching, undertwisting, and relaxation dynamics, Phys. Rev. E 57 (2) (1998) 2134–2149.
[54] T.R. Strick, J.F. Allemand, D. Bensimon, A. Bensimon, V. Croquette, The elasticity of a single supercoiled DNA molecule, Science 271 (1996) 1835–1837.
[55] M.D. Wang, H. Yin, R. Landick, J. Gelles, S.M. Block, Stretching DNA with optical tweezers, Biophys. J. 72 (1997) 1335–1346.
[56] C.J. Benham, Elastic model of the large-scale structure of duplex DNA, Biopolymers 18 (3) (1979) 609–623.
[57] C.J. Benham, S.P. Mielke, DNA mechanics, Annu. Rev. Biomed. Eng. 7 (2005) 21–53.
[58] B.D. Coleman, I. Tobias, D. Swigon, Theory of the influence of end conditions on self-contact in DNA loops, J. Chem. Phys. 103 (1995) 9101–9109.
[59] D. Swigon, B.D. Coleman, I. Tobias, The elastic rod model for DNA and its application to the tertiary structure of DNA minicircles in mononucleosomes, Biophys. J. 74 (1998) 2515–2530.
[60] I. Tobias, D. Swigon, B.D. Coleman, Elastic stability of DNA configurations. I: general theory, Phys. Rev. E 61 (2000) 747–758.
[61] B.D. Coleman, D. Swigon, I. Tobias, Elastic stability of DNA configurations. II: supercoiled plasmides with self-contact, Phys. Rev. E 61 (2000) 759–770.
[62] R. Zandi, J. Rudnick, Constrainst, histones, and 30-nm spiral, Phys. Rev. E 64, Art. No. 051918, 2001.
[63] B. Fain, J. Rudnick, Conformations of closed DNA, Phys. Rev. E 60 (1999) 7239–7252.
[64] B. Fain, J. Rudnick, S. Östlund, Conformations of linear DNA, Phys. Rev. E 55 (1997) 7364–7368.
[65] H. Schiessel, J. Rudnick, R. Bruinsma, W.M. Gelbart, Organized condensation of worm-like chains, Europhys. Lett. 51 (2000) 237–243.
[66] A. Balaeff, L. Mahadevan, K. Schulten, Modeling DNA loops using the theory of elasticity, E-print archive arXiv.org ⟨http://arxiv.org/abs/physics/0301006⟩, 2003.
[67] A. Balaeff, L. Mahadevan, K. Schulten, Structural basis for cooperative DNA binding by CAP and Lac repressor, Structure 12 (2004) 123–132.
[68] B.D. Coleman, W.K. Olson, D. Swigon, Theory of sequence-dependent DNA elasticity, J. Chem. Phys. 118 (2003) 7127–7140.
[69] A.E.H. Love, A Treatise on the Mathematical Theory of Elasticity, Dover, New York, 1944.
[70] S.S. Antman, Nonlinear Problems of Elasticity, Springer, New York, 1995.
[71] J.C. Simo, L. Vu-Quoc, A three dimensional finite-strain rod model. Part II: computational aspects, Comput. Meth. Appl. Mech. Eng. 58 (1986) 79–116.
[72] D.J. Dichmann, Y. Li, J.H. Maddocks, Hamiltonian formulations and symmetries in rod mechanics, in: J.P. Mesirov, K. Schulten, D. Summers (Eds.), Mathematical Approaches to Biomolecular Structure and Dynamics, Springer, New York, 1995, pp. 71–113.
[73] B.D. Coleman, E.H. Dill, M. Lembo, Z. Lu, I. Tobias, On the dynamics of rods in the theory of Kirchhoff and Clebsch, Arch. Ration. Mech. Anal. 121 (1993) 339–359.
[74] D.J. Steigmann, M.G. Faulkner, Variational theory for spatial rods, Arch. Ration. Mech. Anal. 133 (1993) 1–26.
[75] O. Gonzalez, J.H. Maddocks, Extracting parameters for base-pair level models of DNA from molecular dynamics simulations, Theor. Chem. Acc. 106 (2001) 76–82.
[76] S. Goyal, N.C. Perkins, C.L. Lee, Nonlinear dynamics and loop formation in Kirchhoff rods with implications to the mechanics of DNA and cables, J. Comput. Phys. 209 (2005) 371–389.
[77] P.A. Wiggins, R. Phillips, P.C. Nelson, Exact theory of kinkable elastic polymers, E-print archive arXiv.org (arXiv:cond-mat/0409003 v1. 31 August 2004).
[78] Y. Zhou, G.S. Chirikjian, Conformational statistics of bent semiflexible polymers, J. Chem. Phys. 119 (9) (2003) 4962–4970.
[79] Y. Zhou, G.S. Chirikjian, Conformational statistics of semi-flexible macromolecular chains with internal joints, Macromolecules 39 (5) (2006) 1950–1960.
[80] J. McConnell, Rotational Brownian Motion and Dielectric Theory, Academic Press, New York, 1980.
[81] W.T. Coffey, Yu.P. Kalmykov, J.T. Waldron, The Langevin Equation, second ed., World Scientific, Singapore, 2004.
[82] H.P. McKean Jr., Stochastic Integrals, Academic Press, New York, 1969.
[83] A.D. Fokker, Die Mittlere Energie rotierender elektrischer Dipole in Strahlungs Feld, Ann. Phys. 43 (1914) 810–820.
[84] M. Planck, Uber einen Satz der statistischen Dynamik und seine Erweiterung in der Quantentheorie, Sitz. ber. Berlin A Akad. Wiss. 1917 (1917) 324–341.
[85] A.N. Kolmogorov, Uber die analytischen Methoden in der Wahrscheinlich-keitsrechnung, Math. Ann. 104 (1931) 415–458.
[86] C.W. Gardiner, Handbook of Stochastic Methods, second ed., Springer, Berlin, 1985.
[87] H. Risken, The Fokker–Planck Equation, Methods of Solution and Applications, second ed., Springer, Berlin, 1989.
[88] H. Kleinert, Path Integrals in Quantum Mechanics, Statistics and Polymer Physics, second ed., World Scientific, Singapore, 1995.
[89] R.C. Maroun, W.K. Olson, Base sequence effects in double-helical DNA. 2. Configurational statistics of rodlike chains, Biopolymers 27 (1988) 561–584.
[90] W. Miller, Some applications of the representation theory of the Euclidean group in three-space, Commun. Pure Appl. Math. 17 (1964) 527–540.
[91] A.B. Kyatkin, G.S. Chirikjian, Algorithms for fast convolutions on motion groups, Appl. Comput. Harmonic Anal. 9 (2000) 220–241.
[92] D.J. Higham, An algorithmic introduction to numerical simulation of stochastic differential equations, SIAM Rev. 43 (2001) 525–546.
[93] W. Park, Y. Liu, M. Moses, G.S. Chirikjian, Kinematic state estimation and motion planning for stochastic nonholonomic systems using the exponential map, Robotica 26 (4) (2008) 419–434.
[94] N.J. Vilenkin, E.L. Akim, A.A. Levin, The matrix elements of irreducible unitary representations of the group of Euclidean three-dimensional space motions and their properties, Dokl. Akad. Nauk SSSR 112 (1957) 987–989 (in Russian); also N.J. Vilenkin, A.U. Klimyk, Representation of Lie Groups and Special Functions, vols. 1–3, Kluwer Academic Publishers, Dordrecht, Holland, 1991.